

# SUPPLEMENT TO

## Quantifying electric field gradient fluctuations over polymers using ultrasensitive cantilevers

Showkat M. Yazdanian,<sup>1</sup> Nikolas Hoepker,<sup>2</sup> Seppe Kuehn,<sup>1</sup> Roger F. Loring,<sup>1</sup> and John A. Marohn<sup>1</sup>

<sup>1</sup>*Department of Chemistry and Chemical Biology, Cornell University, Ithaca, New York 14853-1301*

<sup>2</sup>*Laboratory of Atomic and Solid State Physics, Cornell University, Ithaca, New York 14853*

(Dated: May 26, 2009; File: SMY`nl-2009-004332`supplement`REVISED)

### I. SUMMARY

We refer the reader to the online Supplement of Ref.1 for detailed information on the apparatus, interferometric displacement detection and interferometer calibration, cantilever frequency detection, and analysis of cantilever ringdown and thermomechanical position-fluctuation data. In Sec. II we summarize the protocol used to calibrate the spring constants of our cantilevers via analysis of cantilever thermomechanical motion. Section III details dielectric spectroscopy measurements of PMMA, PVAc, and PS. In Sec IV we rule out two alternative mechanisms of cantilever frequency fluctuations.

### II. DETERMINATION OF CANTILEVER SPRING CONSTANT

The spring constant  $k_c$  of each cantilever was measured by analyzing thermomechanical position fluctuations using the equipartition theorem, according to the approach of Hutter and Beckhoefer,<sup>2</sup> as follows.

Cantilever position fluctuations,  $\delta x(t)$ , were detected using a calibrated interferometer. A 25-second transient of position fluctuations was recorded and its power spectrum computed. Since the decay time of the cantilever could be as long as a second, it was important to record up to 25 seconds of position-fluctuation data in order to accurately capture the lineshape of the cantilever resonance in the power spectrum. Twenty-five transients were averaged to give a position-fluctuation power spectrum,  $P_{\delta x}$ . A representative power spectrum is shown in Fig. 1(a). The power spectrum was fit to the equation shown in Fig. 1(b) which contains both a thermomechanical contribution and a detector noise floor contribution. The area under the thermomechanical contribution to the power spectrum, equal to  $\langle(\delta x_{th})^2\rangle$ , was computed (with error bars) from fitted parameters as described in Sec. VI of the Ref.1 Supplement.

The spring constant was computed as  $k_c = k_B T / \langle x_{th}^2 \rangle$ . A representative spring constant and associated error is shown in Fig. 1(b):  $8.7 \pm 0.6 \times 10^{-4}$  N/m. An error in spring constant of 5 to 10% is typical.

### III. DIELECTRIC SPECTROSCOPY

Dielectric spectroscopy measurements were made on 450 nm thick PMMA and PVAc films. These measurements required constructing thin-film capacitors of PMMA and PVAc of known area.

Capacitor substrates were constructed from standard quartz wafers by dicing the wafers into 1-inch squares using a commercial wafer dicing saw. The substrate squares were cleaned by repeated ultrasonication in methanol. The squares were loaded into an electron gun evaporator supplied with a custom-made evaporation jig that exposed a 1-inch by 0.5-inch area (Fig. 2(a)). A 50 nm thick layer of aluminum was evaporated onto the quartz substrate at a rate of 0.5 nm/s to create the bottom electrode of the capacitor.

A thin film of PMMA or PVAc was spin cast onto the metallized substrate and annealed as discussed in the paper. The films were removed from the annealing oven and placed in the high vacuum chamber of the electron gun evaporator within

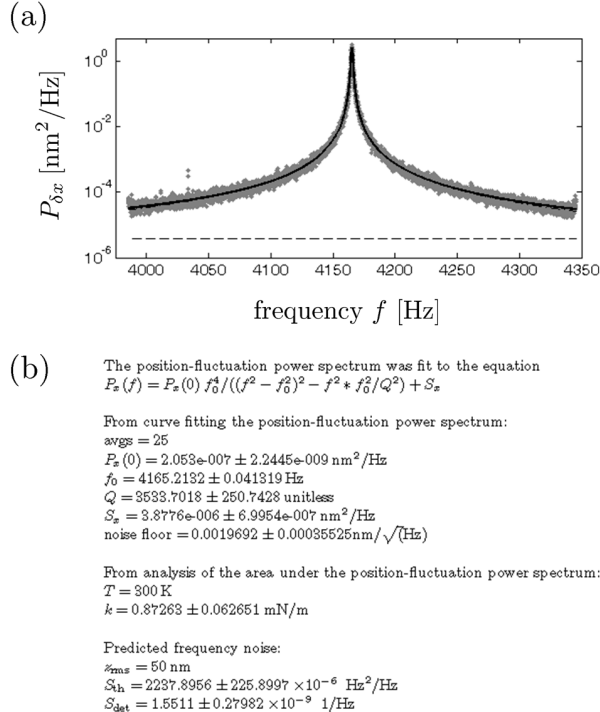


FIG. 1: (a) Power spectrum of cantilever position fluctuations. The solid line is the thermal contribution and the dotted line is the instrument noise floor contribution. (b) Analysis of position fluctuations.

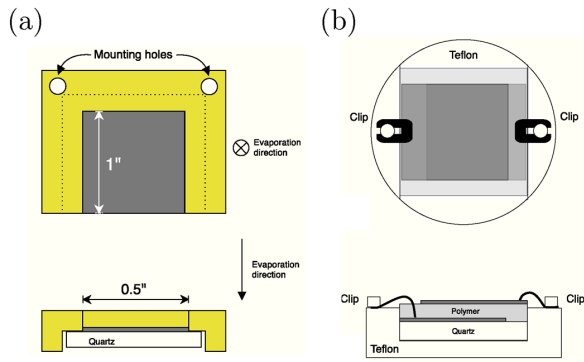


FIG. 2: Dielectric spectroscopy apparatus. (a) A custom brass evaporation jig for making capacitors from polymer thin films on quartz substrates. The actual jig evaporates four substrates simultaneously. Top down view (top): the exposed portion of the quartz substrate is evaporated with a 50 nm aluminum thin film by electron gun evaporation. The mounting holes allow mounting in the evaporator using machine screws. Profile view (bottom): the quartz substrate and the aluminum electrode. (b) Custom dielectric spectroscopy jig for capacitors constructed from thin films. Electrical contacts to electrodes are made with clips which are connected to the leads of the spectrum analyzer. For the low frequency measurements presented here coaxial cables were not necessary.

30 minutes to minimize contamination and water absorption. A second evaporation was then carried out to create the top electrode of the capacitor. Again the jig of Fig. 2(a) was used, but now the substrate was rotated by 180°. To minimize substrate heating, the evaporation rate was kept below 0.1 nm/s so as not to melt the polymer thin film. During this second evaporation, the substrate thermometer did not exceed 17°C. Slow evaporation was especially important for the low- $T_g$  PVAc samples.

The result was a capacitor where top and bottom electrodes could be independently contacted with clips, as shown in Fig. 2(b). The capacitor had a total area of  $A = 0.5 \text{ in} \times 0.75 \text{ in} = 2.4 \times 10^{-4} \text{ m}^2$  and an electrode separation set by the thickness of the spin-cast polymer film. Several devices were sacrificed to check that evaporation of the second electrode did not alter the film thickness and to check the overall thickness of the devices by profilometry. Attempts were made to construct capacitor electrodes by sputtering gold, since sputtering gold electrodes required only a few minutes instead of the 2 hours required to sputter aluminum electrodes. Disappointingly, gold electrodes shorted without exception. This failure was presumably the result of penetration of the gold into the polymer during evaporation or a consequence of the high mobility of gold within the polymer film at room temperature. Aluminum electrodes were unshorted 90% of the time.

A commercial impedance analyzer (Hewlett Packard; Model No. 4192 A LF) was used to measure the real portion of the capacitance and the loss tangent, defined as

$$\tan \delta = \frac{C''}{C'} = \frac{\epsilon''}{\epsilon'}. \quad (1)$$

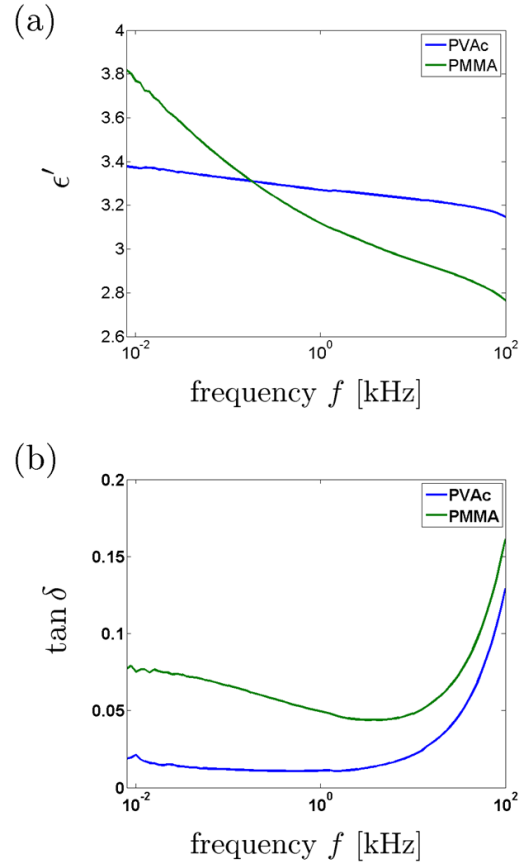


FIG. 3: Dielectric spectra of PMMA and PVAc: (a) real part of the relative dielectric constant and (b) loss tangent.

The observed (real) capacitance  $C'(f)$  was converted to (real) dielectric constant  $\epsilon'(f)$  using the parallel-plate-capacitor formula and the known area of the electrodes and the measured thickness of the polymer film. We constructed three copies of PMMA and PVAc capacitors and measured each using the impedance analyzer. There was approximately a 10% variation in the measured values across the three capacitors for both PMMA and PVAc. This variation is likely due to variation in the film thickness and possibly the metal roughness. These measurements were averaged to produce the resulting spectra shown in Fig. 3.

We believe that the rise of  $\tan \delta$  at high frequency apparent in Fig. 3(b) is an artifact of the lead capacitance. The lead capacitance can be compensated for (W. Scaife and G. McMullin, *Meas. Sci. Technol.*, **5**, 1576 (1994)), but this would have required measuring the lead capacitance independently, which we did not do. The error introduced by the lead-capacitance artifact in the frequency range of interest, 5 to 500 Hz, is less than 10% — smaller than the sample-to-sample variation in capacitance and therefore negligible.

Capacitors with dielectric layers of polystyrene were also constructed. The sensitivity of the Hewlett Packard 4192 A LF impedance analyzer was unfortunately not sufficient to measure the very low losses in polystyrene ( $\tan \delta \leq 0.001$ ).

Professor Ranko Richert of Arizona State University kindly provided us with the room temperature dielectric spectrum of polystyrene. The polystyrene had a weight-averaged molecular weight of  $M_w = 181,000$  g/mol and a polydispersity of  $M_w/M_n = 1.03$ . In the 1 to 100 Hz range, the average values for the dielectric constants are  $\epsilon' = 2.82$  and  $\epsilon'' = 5 \times 10^{-4}$ . The data was measured in the course of doing work for the following paper, but the spectra were not published: "Orientation and Dynamics of Chainlike Dipole Arrays: Donor-Acceptor-Substituted Oligophenylenevinyls in a Polymer Matrix," C. Former, H. Wagner, R. Richert, D. Neher, and K. Müllen, *Macromol.*, **32**, 8551 – 8559 (1999).

#### IV. RULING OUT ALTERNATIVE CANTILEVER FREQUENCY FLUCTUATION MECHANISMS

In addition to the mechanism of eqs 2 and 4–6 of the manuscript, Yazdanian *et al.*<sup>1</sup> identified additional possible frequency noise sources. While the excellent agreement between theory and experiment seen in Fig. 5 of the manuscript strongly suggests that these additional sources are negligible, we have carried out further experiments and calculations to show why this is so.

##### A. Pendulum Terms

If, instead of approximating the cantilever tip as moving perfectly parallel to the surface, the cantilever is treated as a pendulum, then the frequency fluctuation picks up two more terms which depend on additional electric field and electric field gradient components<sup>3</sup>:

$$\delta f_c(t) = -\frac{q_c f_c}{2k_c} \left( \delta \mathcal{E}_{xx}(t) - \frac{\delta \mathcal{E}_z(t)}{L_{\text{eff}}} - 2\theta \delta \mathcal{E}_{zx}(t) \right) \quad (2)$$

Here  $\theta$  is the angle between the cantilever's length vector and the sample's surface normal and  $L_{\text{eff}}$  the effective length of the cantilever, equal to  $1.377L$  for a singly clamped beam such as our cantilever.<sup>4</sup> The second term is much smaller than the first term as long as the tip-sample separation is much less than the cantilever length,  $d \ll L_{\text{eff}}$ , which is the case here. Since we can align the cantilever with an accuracy of  $\pm 0.5^\circ$ ,  $|\theta| \leq 0.009$  radian, and the third term is likewise negligible.

##### B. Anharmonic Potential Terms

If the cantilever's potential energy contains an anharmonic perturbation, then force fluctuations acting in concert with the anharmonic potential lead to additional frequency noise.<sup>1</sup> An anharmonicity could arise from intrinsic cantilever nonlinearities or, alternatively, from tip charge interacting with the field derivative  $\partial^2 E_x / \partial x^2$  expected to be present near a film of randomly oriented dipoles. Therefore an anharmonicity could be a function of both sample composition and tip-sample separation height. To measure the anharmonicity, we note that

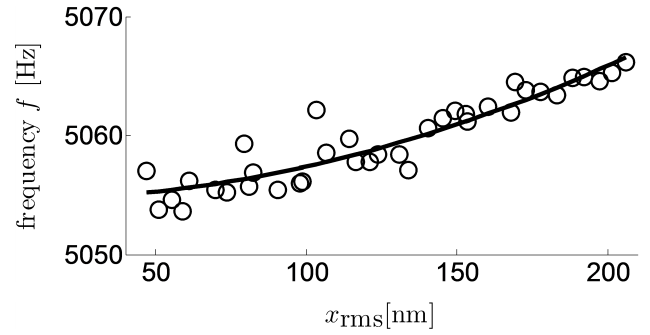


FIG. 4: The dependence of cantilever frequency on drive amplitude at height  $d = 50$  nm over a 40 nm thick PMMA film with  $V_s = 0.5$  V +  $\phi$  with  $\phi = 0.8$  V. The line is a best fit to eq. 4.

adding a cubic term  $V_a = -\alpha x^3/6$  to the potential energy of a harmonic oscillator leads to a negative fractional frequency shift which depends on oscillator drive amplitude according to<sup>5</sup>

$$\frac{\Delta f_c}{f_c} = -\frac{5}{24} \left( \frac{\alpha x_{\text{rms}}}{k_c} \right)^2. \quad (3)$$

Figure 4 presents a measurement of cantilever frequency as a function of drive amplitude for a charged cantilever at a height  $d = 50$  nm over a 40 nm thick PMMA film. Because the frequency in figure 4 increases rather than decreases with amplitude, we conclude that the frequency dependence does not stem from a cubic, but rather from a quartic (or higher order) perturbation to the cantilever potential. A quartic perturbation,  $V_b = \beta x^4/4$ , results in a frequency shift<sup>6</sup>

$$\frac{\Delta f_c}{f_c} = \frac{3}{4} \frac{\beta x_{\text{rms}}^2}{k_c}. \quad (4)$$

Fitting the data in figure 4 to eq. 4, we find  $\beta/k_c = 7 \times 10^{-8}$  nm<sup>-2</sup>. To quantify this perturbation, we compare the energy of the anharmonic term to that of the unperturbed (harmonic) potential energy  $V_h = k_c x^2/2$ . At the peak of the cantilever oscillation, the ratio of these energies is

$$r_b = \frac{V_b}{V_h} = \frac{\beta x_{\text{rms}}^2}{k_c} \quad (5)$$

For a typical cantilever amplitude of 100 nm<sub>rms</sub>, we find that  $r_b = 7 \times 10^{-4} \ll 1$ . Therefore our cantilever is well represented by a harmonic oscillator. While a measurable cantilever anharmonicity is present near a surface, it appears to be a negligible source of cantilever frequency fluctuations in the polymers studied here.

#### References

- <sup>1</sup> S. M. Yazdanian, J. A. Marohn, and R. F. Loring, *J. Chem. Phys.*, **2008**, *128*, 224706, [url].
- <sup>2</sup> J. Hutter and J. Bechhoefer, *Rev. Sci. Instrum.*, **1993**, *64*, 1868 – 1873, [url].
- <sup>3</sup> T. D. Stowe, K. Yasumura, T. W. Kenny, D. Botkin, K. Wago, and D. Rugar, *Appl. Phys. Lett.*, **1997**, *71*, 288 – 290, [url].

- <sup>4</sup> J. A. Sidles, J. L. Garbini, K. J. Bruland, D. Rugar, O. Züger, S. Hoen, and C. S. Yannoni, *Rev. Mod. Phys.*, **1995**, *67*, 249 – 265, [url].
- <sup>5</sup> H. Goldstein, C. P. Poole, and J. L. Safko, *Classical Mechanics*, Addison Wesley, 2002, p. 545 – 547.
- <sup>6</sup> A. Pathak and S. Mandal, *Physics Letters A*, **2001**, *286*, 261 – 276, [url].